NUTATION DAMPER FOR THE AMPTE-IRM SATELLITE
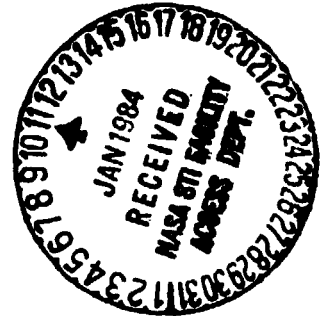## FINAL REPORT

A. Truckenbrodt, B. Schultysik and J. P. Mehltretter

NATIONAL AERONAUTICS AND SPACE ADMINISTRATION
WASHINGTON, DC 20546   APRIL 1983

STANDARD TITLE PAGE

1. Report No. NASA TM-77330	2. Government Accession No.	3. Recipient's Catalog No.
4. Title and Subtitle NUTATION DAMPER FOR THE AMPTE-IRM SATELLITE: FINAL REPORT.		5. Report Date APRIL 1983
		6. Performing Organization Code
7. Author(s) A. Truckenbrodt, B. Schultysik and J. P. Mehltretter		8. Performing Organization Report No.
		10. Work Unit No.
9. Performing Organization Name and Address SCITRAN Box 5456 Santa Barbara, CA 93108		11. Contract or Grant No. NASw-3542
		12. Type of Report and Period Covered Translation
12. Sponsoring Agency Name and Address National Aeronautics and Space Administration Washington, D.C. 20546		14. Sponsoring Agency Code

15. Supplementary Notes

Translation of "Nutationsdämpfer für den
AMPTE-IRM Satelliten: Abschlubericht."
Technology Consulting Institute for Applied
Research GMBH. (West Germany), TC-No. 017-Tru-Scho/sa,
9 Dec. 1982, 20 pp.

16. Abstract

This report describes the design of, computations,
and testing of the nutation damper for the AMPTE-IRM
satellite. Tests were carried out in a pendulum testing
device and the time constants calculated. Findings
showed that the damper remained within the originally
specified values and provided for good dynamic behavior
of the satellite.

17. Key Words (Selected by Author(s))		18. Distribution Statement Unclassified – Unlimited	
19. Security Classif. (of this report) Unclassified	20. Security Classif. (of this page) Unclassified	21. No. of Pages 21	22. Price

TECHNOLOGY CONSULTING

INSTITUTE FOR APPLIED RESEARCH GMBH

TC-No 017-Tru-Scho/sa, 9 Dec 1982

Nutation Damper for the AMPTE-IRM Satellite

Final Report

SUMMARY

This report describes the design of, computations on and testing of the
nutation damper for the AMPTE-IRM satellite. A passive liquid damper has been
developed building on the investigations carried out during the feasibility
study. It consists of a liquid filled O-shaped tube system. The nutational
motions induce liquid oscillations in the tubes; energy is destroyed by
tube friction, constriction of the stream and the formation of turbulence
which naturally is extracted from the satellite movement which is thereby
damped.

The equations of motion (non-linear coupled differential equations
for satellite rotation velocities and the deflections of damping fluid) are
derived for determination of the design parameters; using simulators the
oscillation behaviour can be assessed and the parameters fixed. This design
represents a good compromise with respect to the twelve different satellite
configurations. The attenuation behaviour is evaluated using time constants
(reduction in amplitude to 1/e).

Tests carried out in a pendulum testing device to check out the theory
and to determine friction loss numbers show the anticipated dependency of
the time constants on the respective excitation (= nutation) frequency
and good conformity with the theory.

Along with this, the time constants for the satellite are calculated.
For the design selected (overall length = 572mm, weight = 1165 g, mounting
radius = 375mm) values of 5.6 to 12.3 min result; they are significantly
under the specified value of 30 min. Therefore, from the standpoint of the
nutational motions, the reliable execution of the mission is assured.

* Numbers in the margin indicate pagination of foreign text.

ORGANIZATION

1. INTRODUCTION

The intended objective was the design, manufacture and testing of a
nutation damper for the AMPTE-IRM satellite. In accordance with the results
achieved in the feasibility study, a passive fluid damper was developed.
The emphases of the tasks described in this final report are

a) adaptation of the various damper parameters (dimensions, fluid, etc) to the
specified conditions, that is to:

- 12 different configurations of the satellite (with respect to moments
  of inertia, rotational velocity),
- maximum permissible damping time constants;

b) experimental testing of the theoretical data and the determination of
the important damper parameters.

The satellite configurations and the most important requirements, refer-
ed to the feasibility study, are brought together in the following:

Configurations

Nr.	A	B	C	ω_z	ν
	kg · m²			RPM U/min	
1	174,5	178,0	211,8	60	12,09
2	167,9	171,4	209,5	60	14,08
3	138,4	141,7	201,5	20	8,77
4	152,9	139,4	213,8	20	9,22
5	152,9	166,1	240,4	20	10,12
6	147,9	157,0	229,1	20	10,04
7	146,8	144,0	217,8	20	9,96
8	127,0	124,2	187,1	20	9,79
9	109,0	121,5	171,7	20	9,75
10	105,7	102,9	156,4	20	9,99
11	91,3	100,4	145,0	20	10,22
12	80,2	93,4	133,7	20	10,73

A,B,C are moments of inertia with respect to the main axes x,y,z

ω_z spin velocity

ν nutation frequency of the undamped satellite

4

Requirements

| maximum nutation angles: | $\pm 20^\circ$ for configurations 1,2 |
| | $\pm 3^\circ$ for configurations 3-12 |

residual nutation angle:	$\pm 0.2^\circ$
time constants:	$\tau \leq$ 30 minutes, 15 minutes preferred
weight	$\approx$ 1 kg/damper

2. DESCRIPTION OF THE NUTATION DAMPER   /5/

2.1 Functional Principle

The nutation damper shown in **Figure 1** consists of a closed tube system that is constructed of two long thin tubes ("tube") and two short thick tubes ("cap"). The damper is partially filled with a fluid. Based on the centrifugal acceleration through the rotation (ω_z) around the satellite spin axis, the fluid is located in the tube the furthest removed from the spin axis and in the adjacent areas of the caps. The nutation motions of the satellite excite fluid oscillations in the damper tubes; kinetic energy is destroyed (i.e. converted to heat) through the following effects:

- tube friction of the flowing liquid in the tube
- constriction of the stream by cross-sectional change from cap to tube
- formation of turbulence by stream enlargement through cross-sectional change from tube to cap.

This energy loss is extracted from the satellite such that the nutation motion is reduced.
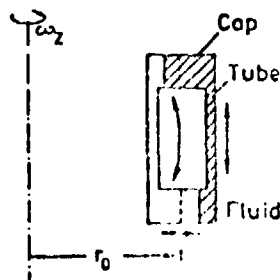

Figure 1   Passive Fluid Nutation Damper

The effectiveness of the damper increases with the amplitude /6/
of the fluid oscillation. For this reason, the best damping effect is achieved in
the case of <u>resonance tuning</u> (i.e. the nutation frequency ν = characteristic
frequency of the fluid oscillation ω_F), see <u>Figure 2</u>. Moreover, one can
see from Figure 2 that in case of increasing damping the effectiveness of the
nutation damper

- falls off in proximity to the resonance point ($\nu/\omega_F \approx 1$, corresponds
  to configurations 3-12)
- increases for frequency ratios $\nu/\omega_F \ll 1$ (corresponds to
  configurations 1 and 2)
- is less strongly influenced by the frequency ratio ν/ω_F .

2.2 Damper Design and Structural Configuration

In order to approach resonance tuning as closely as possible for configu-
rations 3-12, a relationship for the fluid characteristic frequency ω_F to
the spin frequency ω_{zo} of

$$\omega_F/\omega_{zo} = 0.4928$$

was used. This frequency relationship, given a mounting radius r_o = 375mm
is achieved with the following damper geometry: /7/

Tube length	= 472mm
Tube interior diameter	= 19mm
Cap length	= 80mm
Cap interior diameter	= 48.6mm

<u>Figure 3</u> shows the structural form of the nutation damper. Since a
non-magnetic material is required , and on weight grounds as well, the
damper was made of aluminum. Off-the-shelf aluminum tubes were used for the
tubes. Due to the low wall thickness, the tubes and caps were not joined by
welding but by adhesives. For this reason, the caps are fabricated complete
with the couplings needed for the adhesion.

The filling of the damper with the fluid takes place at ambient pres-
sure so that in space an overpressure of 1 bar prevails. Before gluing on
the cover, helium is piped into the damper so that a helium tightness test
can be carried out. An aluminum fixture serves to anchor the damper in
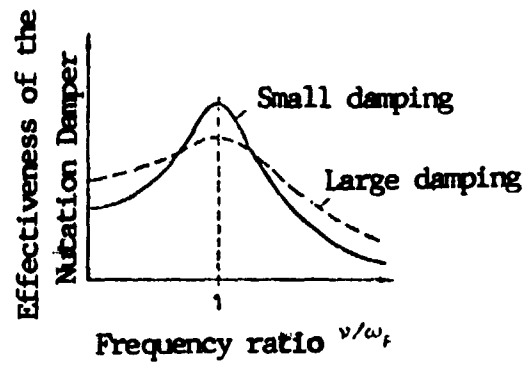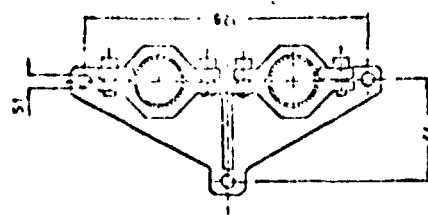the satellite.

Figure 2 : Influence of the Frequency Ratio ν/ω_F and of the Damping on the Effectiveness of the Nutation Damper

In the case of the nutation damper design (Figure 3):

- Overall weight (filled damper with mounting) = 1165 g
- Overall length = 572.2 mm
- Cap outside dimensions: Diameter = 51.6 mm
- Length = 90 mm

The fluid "Flutec PP3" is used to fill the damper:

- Fill level in cap: = 40 mm
- Fluid volume: = 282.2 cm^3

Tube

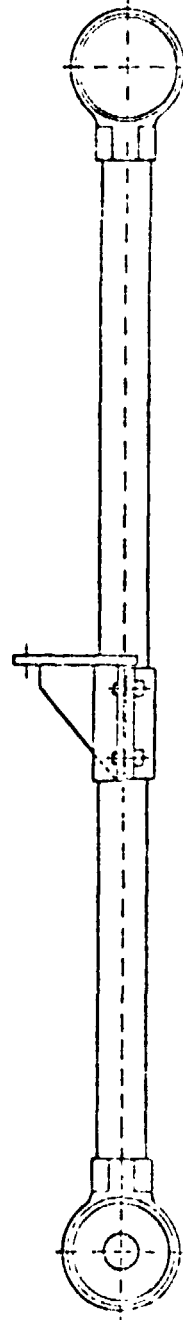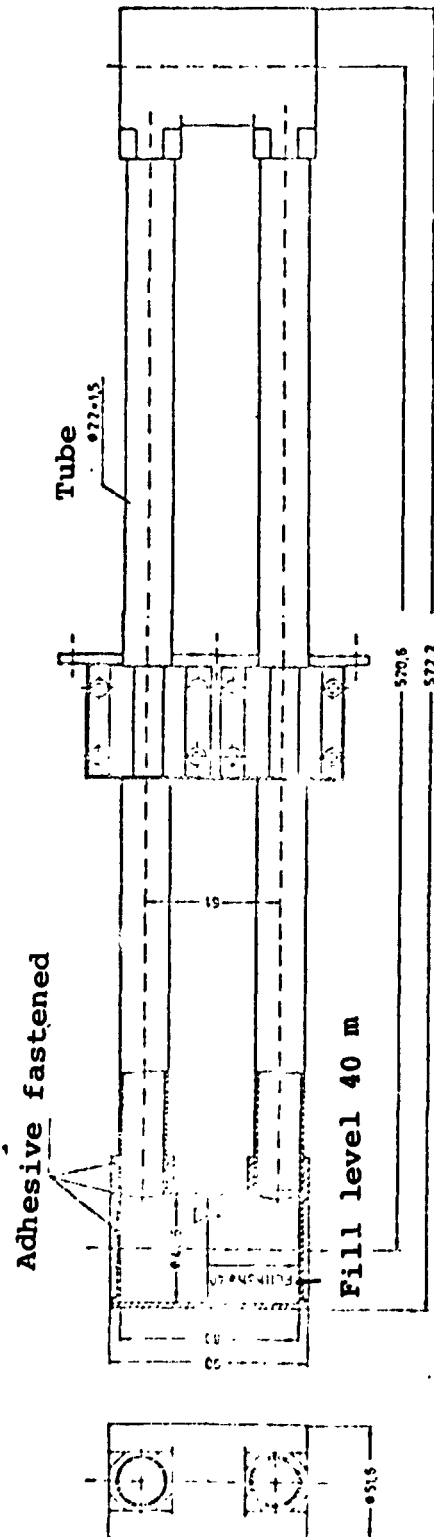Adhesive fastened

Fill level 40 m

Figure 3 : Structural Configuration of the Nutation Damper

3. THEORY

3.1 Equations of Motion

The equations of motion for satellite and damper are contained in the feasibility study in linearized form. For an accurate estimate of the influence of the non-linearities, the general equations of motion were derived for the coordinates

$$\underline{x} = \left[\underbrace{\omega_x \;\; \omega_y \;\; \omega_z \;\; \dot{z}_1 \;\; \dot{z}_2}_{\underline{y}^T} \;\; \vdots \;\; \underbrace{z_1 \;\; z_2}_{\underline{z}^T} \right]^T \tag{1}$$

(ω = satellite rotational velocities, z_1, z_2 fluid deflection in tubes 1,2); in general written form they read:

$$\underline{M}(\underline{x}) \; \dot{\underline{y}} + \underline{f}(\underline{y}, \underline{z}) = \underline{0} \tag{2}$$

$$\dot{\underline{z}} = \underline{E} \; \underline{y}$$

$$\text{mit } \underline{E} = \begin{bmatrix} 0 & 0 & 0 & 1 & 0 \\ 0 & 0 & 0 & 0 & 1 \end{bmatrix} \tag{3}$$

Here, in addition to the laminar tube friction, energy losses were also taken into account which are caused by the in and out streaming from tube into cap (stream constriction, turbulence formation) and turbulent tube friction (alternatively to the laminar tube friction), all in the interest of broadening the description of the energy removal used in the feasibility study.

For the energy loss of a damper it is thus found, see equation (13) in the feasibility study, that

$$\left| \frac{dE}{dt} \right| = \rho \, A_T \, \ell \cdot \left[2 \, \delta \, \dot{z}_1^2 + \frac{\zeta}{2 \, T} \, \dot{z}_1^3 \right] \tag{4}$$

with the loss term ζ , which is only experimentally determinable. The damper

equations must therefore, in accordance with equation (13) of the feasibility study, be supplemented by the terms

$$\frac{1}{2\ell} \cdot \zeta \cdot \dot{z}_1^2 \cdot \text{sgn} \; \dot{z}_1$$

Estimations with $\zeta = 2$ show that the energy loss characterized by ζ is /10/ excessive at large nutation amplitudes. It decreases quadratically with decreasing amplitude in favor of the linear term of the laminar tube friction.

3.2 Time Constants

On account of the non-linearity of the equations of motion, the amplitude history is no longer characterized by an exponential function with constant exponents. Therefore, it is impossible to define time constants independent of the amplitude. Equally, a sufficiently accurate energy-sink approximation is no longer possible. Therefore, the "theoretical" time constants are ascertained by the following procedure:

    1. Simulation of complete non-linear equations of motion

    2. Conversion of the amplitude term ΔA after an "examination period" Δt into an equivalent exponential function or time constant

$$\Delta A = e^{-\Delta t/\tau} \tag{5}$$

    3. Time constant

$$\tau = -\Delta t / \ln \Delta A \tag{6}$$

The time constants derived with this procedure are collated in Section 5.

4. TEST DEVICE

Damping tests were carried out with

● plexiglass nutation dampers with various filling levels

● the ultimate flight model

to check the theory and to experimentally determine the loss term ζ; these were done using the test device described in the feasibility study. With the plexiglass dampers, the stream processes could be clearly observed.

The test mechanism (Figure 4) consists of a pendulum (total mass m_{ges}) /11/ suspended at point A. By displacement of the pendulum tube (m_R) and of the weights m_G, the center of gravity interval s and the moment of inertia Θ_A can be changed with respect to the support point A. In this way the period of oscillation T of the pendulum can be changed.

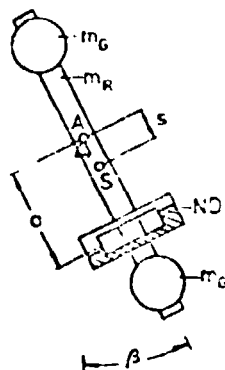$$T = 2\pi \sqrt{\frac{\Theta_A}{m_{ges} \cdot g \cdot s}}$$

11

Figure 4 : Test Mechanism for Nutation Damper

The nutation damper ND is fixed on the pendulum at interval a from the pivot A.

At different pendulum geometries, (i.e. different characteristic frequencies of the pendulum), the oscillation behaviour for an initial amplitude of $\beta_0 = 15^O$ was recorded with a rotary potentiometer and recorder both with and without the nutation damper. Without the nutation damper the effect of bearing friction and air resistance is determined. The time constants amount here to about 200 to 850 sec depending on the pendulum moment of inertia. In the measurements with the nutation damper, the interval a was set at: $a = 375mm = r_o$, corresponding to the installation in the satellite.

From the time constants measured for air resistance and bearing friction /12/ τ_{L+L} (in the case of constant pendulum geometry) and the time constants measured for the nutation damper + air resistance + bearing friction τ_{ND+L+L} follow the time constants $\tau_{P,ND}$ of the pendulum <u>only</u> with the nutation damper:

$$\tau_{P,ND} = \frac{\tau_{ND+L+L} \cdot \tau_{L+L}}{\tau_{L+L} - \tau_{ND+L+L}} \tag{8}$$

Figure 5 shows the time constants of the pendulum thus determined, relative to the potential initial energy of the pendulum.

$$E_{pot,o} = m_{ges} \cdot g \cdot s \cdot (1 - \cos \beta_o) \qquad (9)$$

It is recognized that the effectiveness of the nutation damper is at its greatest (i.e. smallest time constant) when the pendulum (= excitation) frequency f_p coincides with the characteristic frequency f_E of the fluid oscillation. The characteristic frequency on earth amounts to

$$\nu_E = \sqrt{\frac{2g}{b + l_T \cdot \frac{A_c}{A_T}} - \left(\frac{4 \pi \nu_{FL}}{A_T \cdot (1 + \frac{A_T}{A_c} \cdot \frac{b}{l_T})} \right)^2} \rightarrow f_E = 23,76 \text{ oscillation/min.}$$

In contrast, in space there follow:

in configurations 1 and 2 : f_E = 29.568 oscillations/min

in configurations 3-12 : f_E = 9.856 " "

Thus, in space the relationship between the nutation frequency ν and /13/ the characteristic frequency f_E amounts to

in configurations 1 and 2 : ν /f_E = 0.41-0.48

in configurations 3-12 : ν /f_E = 0.89-1.09

These frequency ratios w re achieved on the test mechanism (on earth) with the pendulum frequencies

$$f_p = 9.7 - 11.4 \text{ osc./min.} \,\,\hat{=}\,\, \text{configurations 1 and 2}$$

$$f_p = 21.1 - 25.9 \text{ osc./min.} \,\,\hat{=}\,\, \text{configurations 3-12}$$

corresponds to
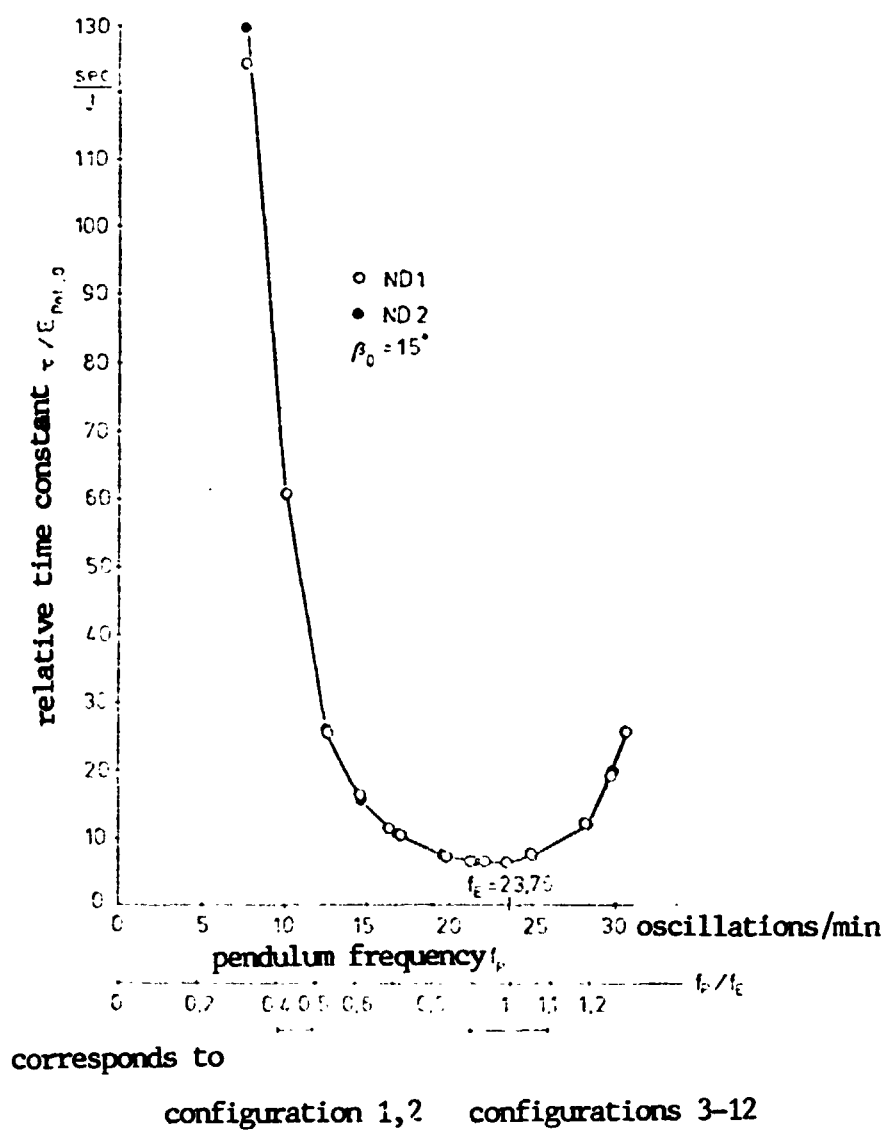
configuration 1,2   configurations 3–12

<u>Figure 5</u> : Time Constants of the Test Mechanism Pendulum, relative to the potential initial energy, as a function of pendulum frequency.

14

Both the identically constructed nutation dampers of the satellite ("ND 1"   /14/
and "ND 2" were used in the measurements on the test mechanism. It is recognized
that the findings on both nutation dampers correspond well, as would be
expected. Moreover, the limited deviations indicate that measurement and
evaluation errors in the investigations on the test mechanism are also small.

To determine the loss term ζ, the experimentally determined time constants
for the test mechanism were compared with the time constants computed for
the test mechanism. Here it is shown that with ζ =2.2 a very good agreement
is achieved between computation and measurement (error about 1.5- 4%) in the
neighborhood of the resonance point, that is for f_p/f_e = 0.9-1.1. For the
frequency ratio f_p/f_E= 0.4-0-5,an optimum value ζ = 4.9 follows. These
different ζ values make it clear that in the resonance case and with
subcritical excitation, different stream conditions are present in the nuta-
tion damper.

5. TIME CONSTANTS FOR THE SATELLITE

With the numerical values that apply to the satellite, the time constants
shown in Figure 6 result, as a function of satellite configuration. An initial
nutation angle of β_0 =20° was used in configurations 1 and 2 for the com-
putations and of β_0 = 3° in the succeeding configurations 3-12. The values
ascertained experimentally on the test mechanism were used for the loss
term ζ , that is:

configurations 1 and 2: ζ =4.9
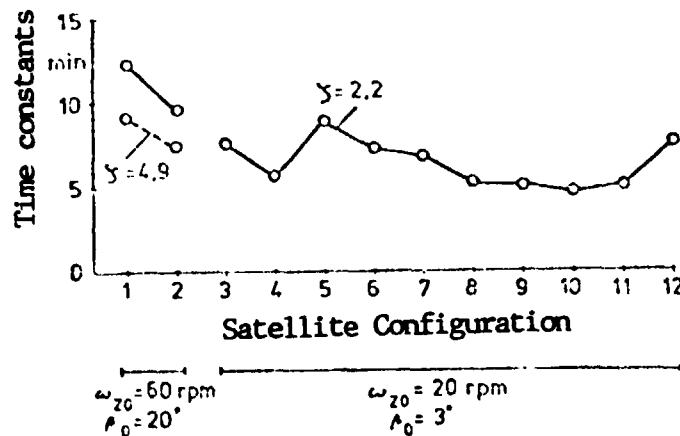configurations 3-12   : ζ =2.2

/15/

Figure 6 : Computed Time Constants for Different Satellite Configurations

It is seen that in all configurations the time constant lies between about 5 and 12 minutes. In configurations 1 and 2, the higher ζ value produces an improvement, because at a subcritical excitation the effectiveness of the nutation damper is improved with an increase in ζ (see **Figure 2**). For comparison, computations were also carried out in configurations 1 and 2 using $\zeta = 2.2$. In this way the range of time constants which result during the reduction of a large initial nutation angle down to a small final angle is limited. For configurations 3-12 (i.e. for $\nu/f_E \approx 1$) one can expect an even faster damping at very small nutation angles because then the influence of the turbulence damping is smaller and near the resonance point a more effective damping is achieved with the tube friction (see **Figure 2**).

In **Figure 7** are shown the final nutation angles after a total damping time of $t_{ges} = 1000$ sec, when the initial nutation angle in configurations 1 and 2 $\beta_0 = 20^O$ and in configurations 3-12, $\beta_0 = 3^O$.
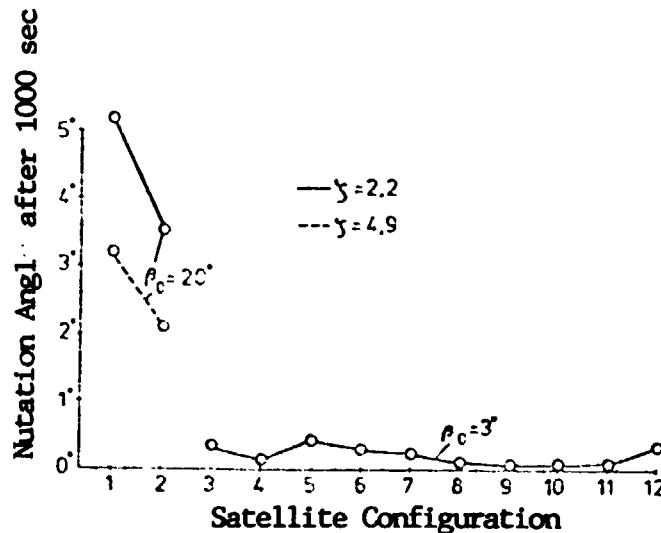
/16/

Figure 7: Nutation Angle of the Satellite after 1000 sec for the Different Satellite Configurations

Figure 8 shows for the different configurations the maximum initial nutation angle which results in a final nutation angle of $\beta_{.1000 \; sec} = 0.2°$, after a damping time of 1000 sec.
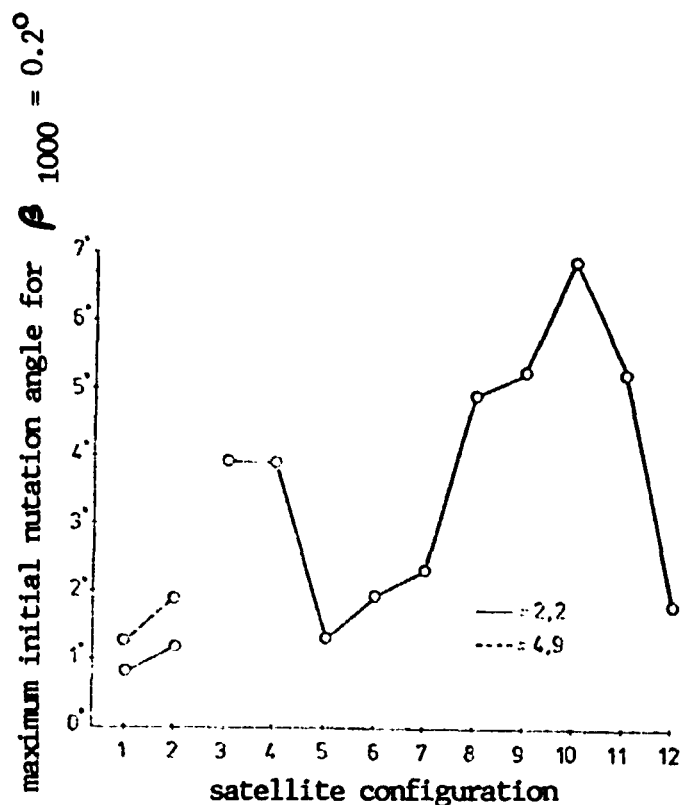

Figure 8 : Maximum Initial Nutation Angle with which after 1000 sec a Nutation Angle of 0.2° is Achieved, for the Different Satellite Configurations

17

Figure 9 shows , using the relatively unfavorable example of configuration /17/
5 (see Figure 6), that with a change in the characteristic value ζ , the computed time constant of the nutational motion of the satellite remains about
in the same order of magnitude. This means that the time constants calculated for
the satellite remain approximately correct, even when the actual characteristic
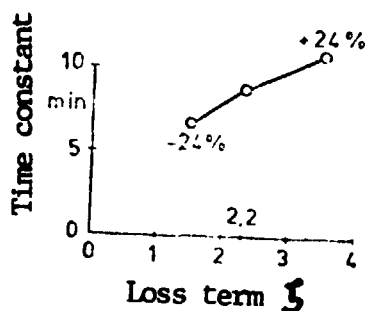value ζ occurring in space deviates somewhat from the value developed on the
test device.

Figure 9 : Influence of the Loss Term ζ on the Time Constant of the
Satellite (Example in Configuration 5)

18

With this it is shown that the damper clearly remains within the originally specified values, also estimated in the feasibility study, and accordingly it can provide for good dynamic behavior of the satellite.
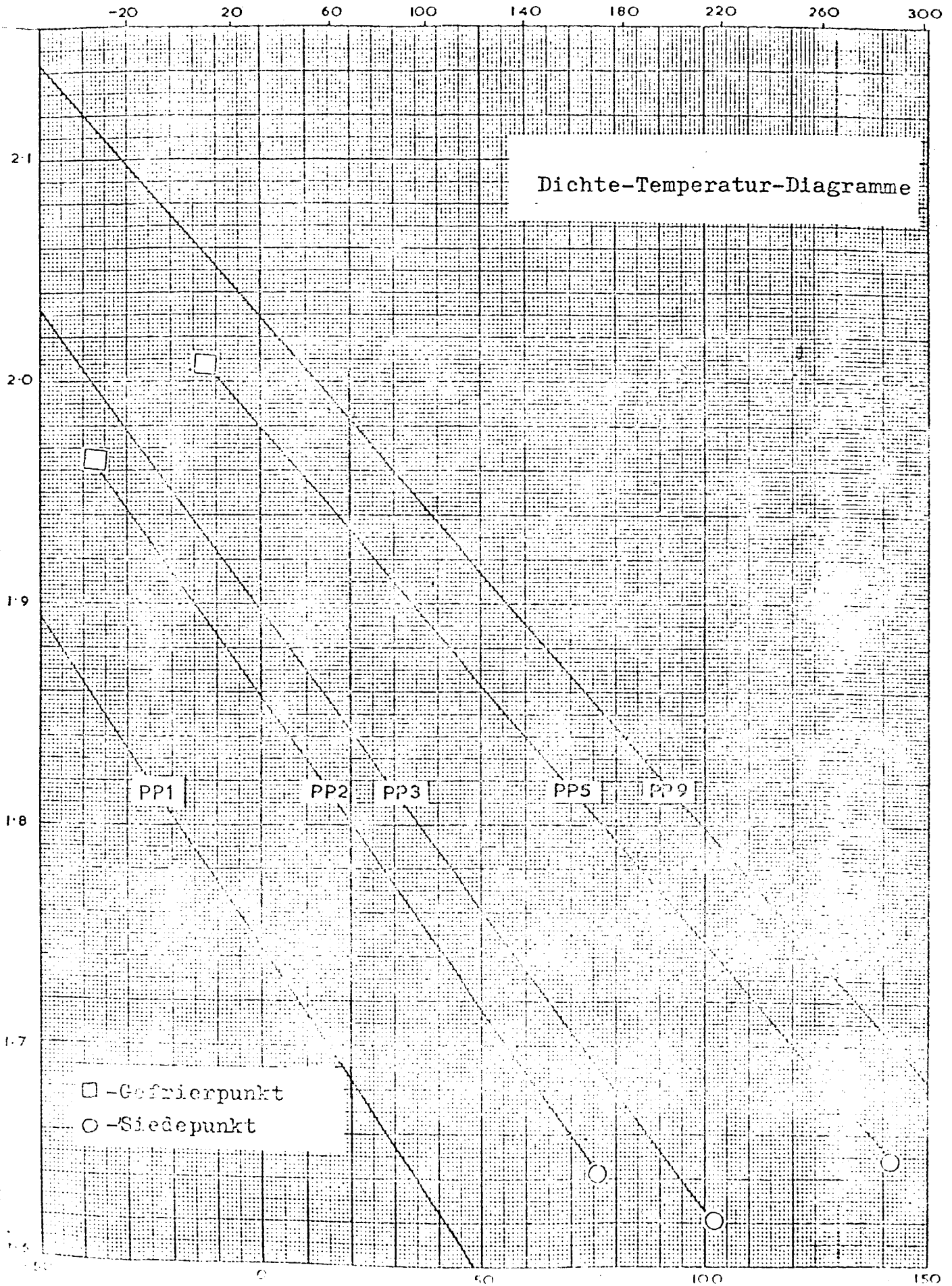
Temperatur (°F)

Dampfdruckdiagramme

PPSO   PP1   PP2   PP3   PP5   PP9

□ –Gefrierpunkt
△ –Krit. Temperatur
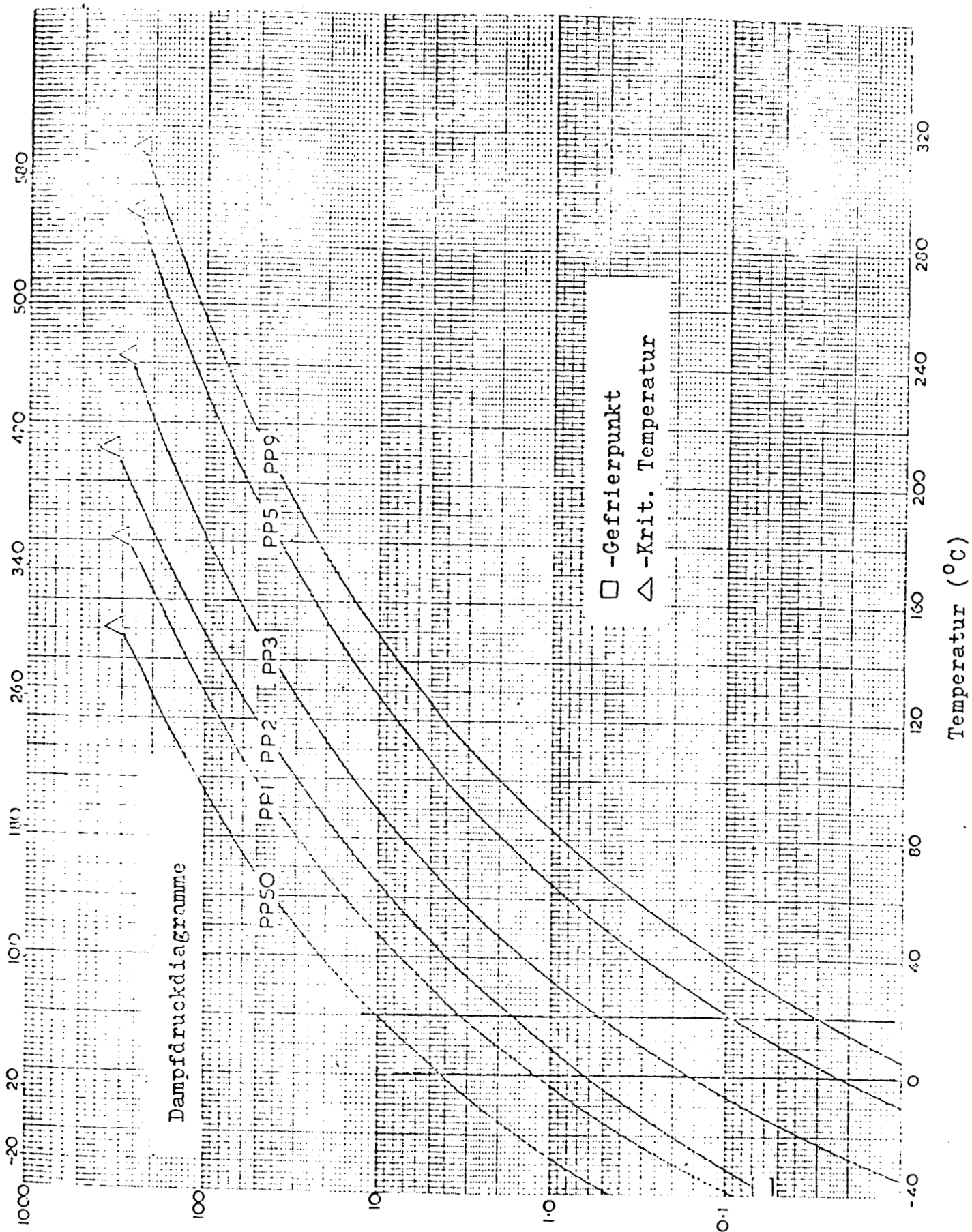
Temperatur (°C)

Druck (absolut) in P.S.I.A.

1 P.S.I.A. = 0,0681 atm

1 atm = 14,68 P.S.I.A.

Dichte (g/cm^2)

Dichte-Temperatur-Diagramme

2·1

2·0

1·9

PP1   PP2   PP3   PP5   PP9

1·8

1·7

□ –Gefrierpunkt
O –Siedepunkt

1·6

Viskositätsdiagramme

Temperatur (°F)

Temperatur (°C)

PP 9

PP 5

PP 3

PP 2

PP 1

□ -Gefrierpunkt

○ -Siedepunkt

20